Ultra-broadband Tapered Slot Terahertz Antennas on Thin Polymeric Substrate

Masami Inoue[#], Masayuki Hodono[#], Shogo Horiguchi[*],
Masayuki Fujita[*], and Tadao Nagatsuma[*]

[#] Functional Design Technology Center, Nitto Denko Corp., Suita, Osaka 565-0871, Japan
[*] Graduate School of Engineering Science, Osaka University, Toyonaka, Osaka 560-8531, Japan

Abstract— **We developed a planar tapered slot antenna on a thin polymeric substrate with low dielectric constant for terahertz-wave applications. The efficiency and the gain of this antenna are not degraded even for higher frequencies. Due to the ultra-broadband features, we demonstrate multiband terahertz wireless error-free communications at 1.5 Gbits/s for both 120 and 300 GHz bands.**

I. INTRODUCTION

Research that explores terahertz (THz) waves at frequencies from 100 GHz to 10 THz has recently attracted much attention, especially since THz waves are suited to such novel applications as spectroscopic sensing, non-destructive imaging, and ultra-broadband wireless communications [1-5]. Planar antennas fabricated on semiconductor substrates have attracted great interest for THz applications [6-16], because planar structures offer great potential for integration with other planar devices. Here, as a planar antenna, we focus on a tapered slot antenna, which is a kind of traveling-wave antenna, that can achieve ultra-broadband operation since it has no resonance at a specific frequency. However, serious practical problems exist: the antenna gain decreases, and the antenna pattern diverges due to unnecessary substrate modes that are excited when the substrate thickness is increased against the wavelength of interest [16-19]. At THz-wave frequencies, the wavelength becomes less than one millimeter, and then this problem becomes remarkable.

In this paper, we present our recent progress in the development of ultra-broadband planar antennas fabricated on a polymeric substrate. We investigate both the theoretical and experimental performances of tapered slot antennas at sub-THz frequencies. We also describe wireless transmission experiments using a receiver module integrated with an antenna that can be operated at both 120 and 300 GHz.

II. ANTENNA STRUCTURE AND SIMULATIONS

Figure 1 shows a schematic of the tapered slot antenna studied in this work. It consists of a substrate, a copper (Cu) pattern, and is nickel (Ni)-gold (Au) plated. THz waves are detected or radiated at the wider edge of the tapered slot. Such semiconductor substrates as indium phosphide (InP) have so far been used in transmitter and receiver modules [11-16]. However, the high relative dielectric constant ε_r of these substrates, typically 12, deteriorates the radiation efficiency and the antenna directivity, because the electromagnetic-wave radiation is attracted to the semiconductor substrate when the frequency increases [16, 19]. To overcome this problem, we proposed a tapered slot antenna on a polyimide film with a ε_r as low as 3 [20, 21].

To compare the semiconductor and polymeric substrates, we changed the dielectric constant and the thickness in the simulation. Table I summarizes the material properties of the substrates. The simulations were performed by a finite-element method considering the dielectric loss tangent (tanδ) and conductivity σ of the metal layers.

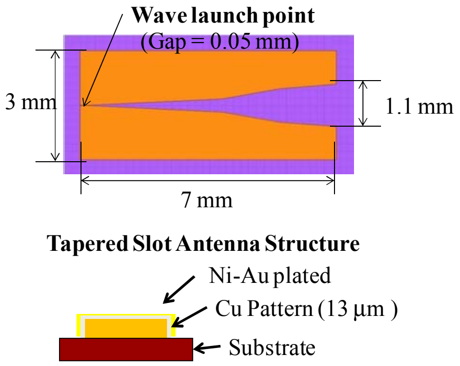

Fig. 1 Schematic of a tapered slot antenna. Conductivities of Cu, Ni, and Au are set to 5.80×10^7 S/m, 1.45×10^7 S/m, and 4.10×10^7 S/m, respectively.

TABLE I
Material characteristics of substrate

Material	Dielectric constant (ε_r)	tanδ	Thickness [µm]
InP	12.4	0.007 (@1GHz)	100
Polyimide	3.2	0.0105 (@1MHz)	25

The simulated electric-field distributions at 300 GHz are shown in Fig. 2. The antenna on a 25-µm-thick polyimide substrate produces a good radiation level. On the other hand, when a 100-µm-thick InP substrate is used, the THz wave is confined to the substrate due to its high dielectric constant. Although the thickness of the InP substrate must be reduced to overcome this problem, handling such a fragile InP substrate is very difficult. Thus, using low dielectric constant and thin substrates is essential for tapered slot antennas in THz applications.

Figure 3 shows the antenna pattern of the polyimide and InP substrates for an E-plane at 300 GHz. The maximum gains of the polyimide and InP antennas are estimated to be 12.4 and 6.0 dBi, respectively. The polyimide antenna only radiates toward the tapered slot direction. On the other hand, the antenna InP pattern has many side lobes due to the excitation of the higher order modes inside the high dielectric constant substrate, which is much thicker than the wavelength.

Next we calculated the radiation efficiency for various frequencies (Fig. 4). Radiation efficiency η is defined by

$$\eta = P_{\text{rad}} / \left(P_{\text{rad}} + P_{\text{loss}} \right) \qquad (1),$$

where P_{rad} is the total radiated power and P_{loss} is the dielectric and conductive losses. The efficiency of the polyimide antenna is almost constant and higher than that of the InP one from 100 to 500 GHz. This is because the polyimide substrate hardly affects the propagation of the THz waves. On the other hand, the THz wave is strongly confined by the InP substrate and suffers material losses.

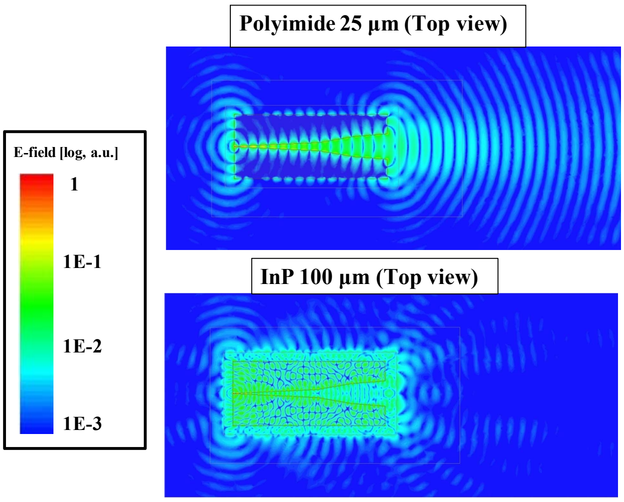

Fig.2 Simulated electric-field intensity distributions at 300 GHz (top view). Upper and bottom figures show 25-μm-thick polyimide and 100-μm-thick InP, respectively.

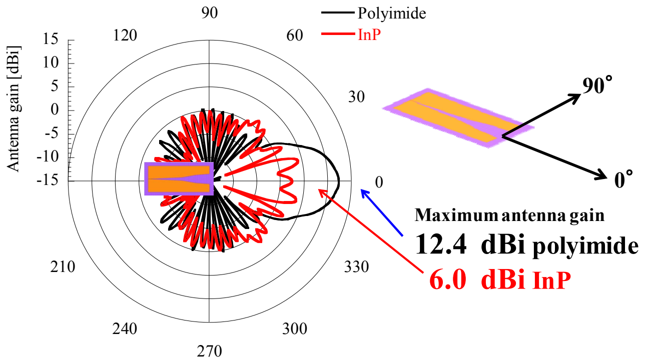

Fig.3 Simulated E-plane antenna patterns for polyimide and InP.

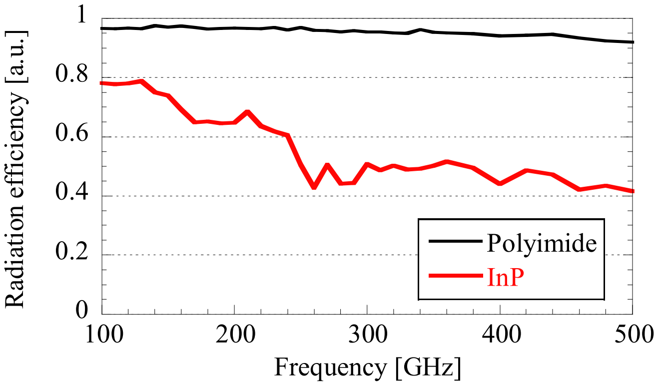

Fig. 4 Radiation efficiency vs. frequency for polyimide and InP.

III. ANTENNA PATTERN MEASUREMENTS

For our experiments, we fabricated a receiver module that consists of a SMA connector, a rigid board, and an antenna on a 25-μm-thick polyimide film layer (Fig. 5). The rigid board is designed to allow air space under the antenna to decrease the effective dielectric constant. A Schottky barrier diode (SBD) chip [22] was mounted on the antenna by flip-chip bonding.

We evaluated the antenna properties by measuring the directional characteristics with a photonics-based transmitter (Fig. 6). In the transmitter, a sinusoidally intensity-modulated optical signal at 120 or 300 GHz is generated by two sets of wavelength-tunable lasers with a wavelength difference of 0.96 or 2.4 nm that corresponds to 120 or 300 GHz, respectively. The optical signal is modulated with an optical intensity modulator at 100 MHz by a signal generator. The optical signal is converted into a THz signal by an ultrafast photodiode [23]. In the receiver module, the detected THz signal is demodulated by the envelope detection, and the demodulated signal is amplified by a pre-amplifier that has a bandwidth of up to 1.5 GHz. The transmission distance was set to 90 mm. Fig. 7 shows the antenna patterns. Our experimental results agree well with the designed ones. Consequently, the polyimide antenna demonstrated a single lobe in the direction of a tapered slot at both the 120- and 300-GHz bands.

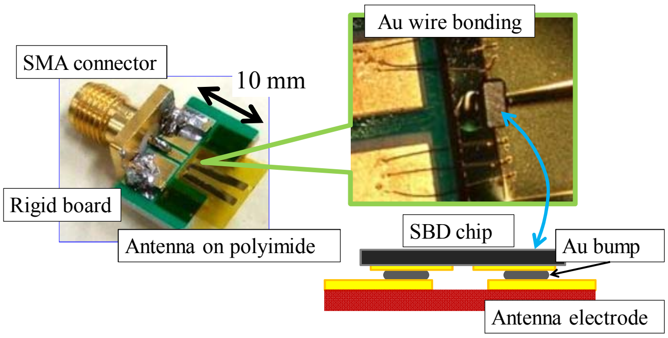

Fig. 5 Receiver module with a tapered slot antenna on polymeric substrate.

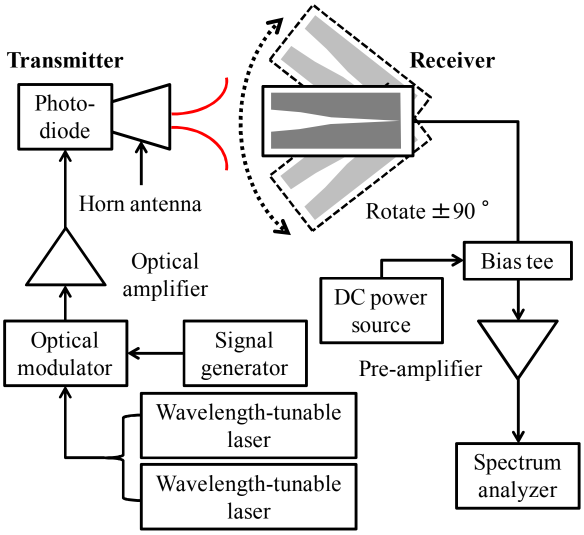

Fig.6 Block diagram of antenna pattern measurements.

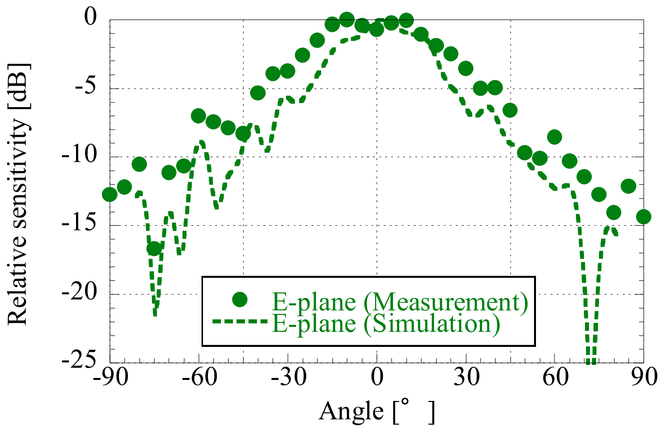

(a) 120 GHz

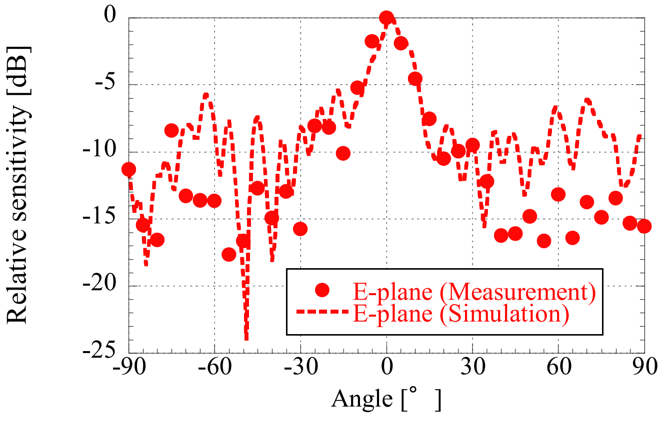

(b) 300 GHz

Fig. 7 Antenna patterns: (a) 120 and (b) 300 GHz.

IV. THz WIRELESS COMMUNICATION

We performed experiments on THz communication for both 120- and 300-GHz bands to demonstrate the ultra-broad property of the antennas. Compared with the set-up in Fig. 6, the optical signal was ON-OFF modulated with an optical intensity modulator, which was driven by the pulse pattern generator. The demodulated signal was reshaped by a limiting amplifier. In addition, we introduced dielectric lenses to collimate the THz waves.

Figure 8 shows the relationship between the photocurrent of the transmitters, which is proportional to the square root of the transmitted power, and the bit-error-rate (BER) for the 120- and 300-GHz carrier frequencies. This result indicates that the transmission power required for error-free transmission for 300 GHz is larger than that for 120 GHz. This is due to the frequency-dependent sensitivity of the SBD chip used in our experiment; the 3-dB bandwidth is around 110 GHz.

Figure 9 depicts eye diagrams at 1.5 Gbit/s for the 120- and 300-GHz bands. Error-free transmission was confirmed not only by the BER tester (BER < 10^{-11}) but also by transmitting uncompressed high-definition television (HDTV) video data (Fig. 10).

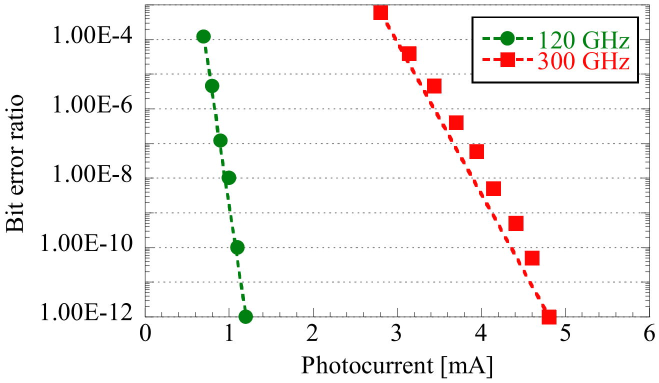

Fig. 8 BER vs. photocurrent for 120 and 300 GHz.

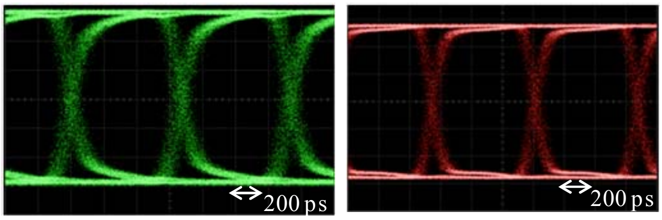

(a) 120 GHz (b) 300 GHz

Fig. 9 Measured eye-diagrams at 1.5 Gbit/s: (a) 120 and (b) 300 GHz.

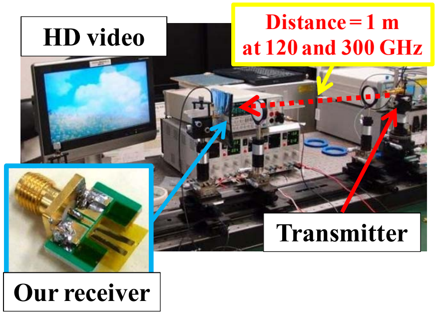

Fig. 10 Experiment for transmitting uncompressed HDTV video data.

V. CONCLUSION

We have developed an ultra-broadband THz antenna using a polymeric substrate. Due to the low dielectric constant of the polymeric substrate, we have successfully demonstrated multiband THz receivers covering frequencies from 100 to 300 GHz bands in antenna pattern measurements and wireless transmission experiments.

ACKNOWLEDGMENTS

The authors thank Yusuke Minamikata and Daiki Tsuji for their experimental support. This work was supported in part by the JST-ANR WITH program and the Strategic Information and Communications R&D Promotion Programme (SCOPE) by the Ministry of Internal Affairs and Communications, Japan.

REFERENCES

[1] M. Tonouchi, “Terahertz technologies: present and future,” Nat. Photonics, vol. 1, no. 2, pp. 97-105, Feb. (2007).

[2] T. Nagatsuma, “Terahertz technologies: present and future,” IEICE Electron. Express, vol. 8, no. 14, pp. 1127-1142, Jul. 2011.

[3] H.-J. Song and T. Nagatsuma, “Present and future of terahertz communications,” *IEEE Trans. THz Sci. Technol.*, vol. 1, no. 1, pp. 256–263, Sep. 2011.

[4] T. Kleine-Ostmann and T. Nagatsuma, “A review on terahertz communications research,” *J. Infrared, Millim. Terahertz Waves*, vol. 32, no. 2, pp. 143–171, Feb. 2011.

[5] J. Federici and L. Moeller, “Review of terahertz and subterahertz wireless communications,” *J. Appl. Phys.*, vol. 107, no. 11, p. 111101-1–111101-22, Jun. 2010.

[6] N. Orihashi, S. Hattori, and M. Asada, “Millimeter and submillimeter oscillators using resonant tunneling diodes with stacked-layer slot antennas,” *Jpn. J. Appl. Phys.*, vol. 43, no. 10A, pp. L1309- L1311, Oct. 2004.

[7] R. Piesiewicz, M. N. Islam, M. Koch, and T. Kürner, “Towards short-range terahertz communication systems: basic considerations”, in *18th International Conference on Applied Electromagnetics and Communications, Dubrovnik, Croatia*, Techn. Digest. p. 153, Oct. 2005.

[8] M. N. Islam and M. Koch, “Terahertz patch antenna arrays for indoor communications,” *Int. Conference on Next-Generation Wireless Systems 2006*, (Dhaka, Bangladesh, 2006).

[9] M. Asada, S. Suzuki, and N. Kishimoto, “Resonant tunneling diodes for sub-terahertz and terahertz oscillators,” *Jpn. J. Appl. Phys.*, vol. 47, no. 6, pp. 4375-4384, Jun. 2008

[10] K. Urayama, S. Aoki, S. Suzuki, M. Asada, H. Sugiyama, and H. Yokoyama, “Sub-terahertz resonant tunneling diode oscillators integrated with tapered slot antennas for horizontal radiation,” *Appl. Phys. Exp.*, vol. 2, pp. 044501-1-044501-3, Apr. 2009.

[11] T. Mukai, M. Kawamura, T. Takada, and T. Nagatsuma, “1.5-Gbps wireless transmission using resonant tunneling diodes at 300 GHz,” *Tech. Dig. Optical Terahertz Science and Technology 2011 Meeting*, MF42, Santa Barbara, 2011.

[12] T. Shiode, T. Mukai, M. Kawamura, and T. Nagatsuma, “Giga-bit wireless communication at 300 GHz using resonant tunneling diode detector,” in *Proc. Asia-Pacific Microw. Conf. (APMC2011),* pp. 1122-1125, Dec. 2011.

[13] T. Shiode, M. Kawamura, T. Mukai, and T. Nagatsuma, “Resonant-tunneling diode transceiver for 300 GHz-Band Wireless Link,” in *Proc. Asia-Pacific Microw. Photon. 2012 (APMP2012)*, WC-1, Kyoto, Apr. 2012.

[14] K. Ishigaki, M. Shiraishi, S. Suzuki, M. Asada, N. Nishiyama, and S. Arai, “Direct intensity modulation and wireless data transmission characteristics of terahertz-oscillating resonant tunnelling diodes,” *Electron. Lett.*, vol. 48, no. 10, pp. 582-583, May. 2012.

[15] A. Kaku, T. Shiode, T. Mukai, K. Tsuruda, M. Fujita, and T. Nagatsuma, “Characterization of resonant tunneling diodes as receivers for terahertz communications,” *Int. Sympo. Frontiers in THz Technology (FTT2012)*, Nara, no. Pos1.51, Nov., 2012.

[16] A. Kaku, T. Shiode, T. Mukai, K. Tsuruda, M. Fujita, and T. Nagatsuma, “3-Gbit/s error-free terahertz communication using resonant tunneling diode detectors integrated with MgO hyper-hemispherical lens,” *Asia-Pacific Microwave Photonics Conference (APMP2013)*, Gwangju, no. MD-1, Apr. 2013.

[17] K. S. Yngvesson *et al*, “The Tapered Slot Antenna - A new integrated element for mm wave applications,” *IEEE Trans.Microwave Theory and Tech.*, 37, 2, pp. 365-374, Feb. 1989.

[18] G. M. Rebeiz, “Millimeter-wave and terahertz integrated circuit antennas,” *Proc. IEEE*, vol. 80, no. 11, pp.1748-1770, Nov. 1992.

[19] K. S. Yngvesson, T. L. Korzeniowski, Y. S. Kim, E. L.Kollberg, and J. F. Johansson, “The tapered slot antenna-A new integrated element for millimeter-wave applications,” *IEEE Trans. Microw. Theory Tech.*, vol. 37, no. 2, pp. 365–374, Feb. 1989.

[20] M. Inoue, M. Hodono, S. Horiguchi, K. Arakawa, M. Fujita and T. Nagatsuma, “Ultra-broadband Receiver for Multiband Terahertz Communications,” *International Workshop on Optical Terahertz Science and Technology 2013 (OTST 2013)*, Kyoto, F2B-2, Apr., 2013.

[21] M. Inoue, M. Hodono, S. Horiguchi, K. Arakawa, M. Fujita, and T. Nagatsuma, “Ultra-broadband receivers using polymeric substrate for multiband terahertz communications,” *2013 International Symposium on Electromagnetic Theory (EMTS2013)*, Hiroshima, May, 2013.

[22] L. Liu, J. L. Hesler, X. Haiyong, A.W. Lichtenberger, and R.M. Weikle, “A broadband quasi-optical terahertz detector utilizing a zero bias schottky diode,” *IEEE Microw. Wireless Comp. Lett.*, vol. 20, no. 9, pp. 504-506, Sept. 2010.

[23] T. Nagatsuma, H. Ito, and T. Ishibashi, “High-power RF photodiodes and their applications,” *Laser Photon. Rev.*, vol. 3, pp. 123–137, no. 1-2, Feb. 2009.